Nonlinear Re-entry Motion of a Towed Wire

Henry R. Busby,* David H. Smith,† and David F. Bremmer†
Prototype Development Associates, Inc., Santa Ana, Calif.

Wires towed behind re-entry vehicles fail in tension due to the combined effects of aerodynamic drag and heating. Such wires experience a damped periodic motion that is essentially two-dimensional. Since both aerodynamic forces and heating are proportional to deflection, it is necessary to determine the decay of the periodic motion to analyze the survival of such a wire. In this paper the principle of virtual work is used to define the large deflection planar motion of a thin, straight, uniform cross-section elastic wire. The wire is assumed to have one end fixed and the other end free and to be subjected to time-varying deflection dependent aerodynamic forces distributed along its length. Two methods of treating the free end boundary conditions are investigated, and both methods are found to provide a good correlation of laboratory measurements of free vibration. Using these methods it is found that over the altitude range from 1000 to 350 kft, some wires of interest are predicted to remain essentially straight, so that their predicted motion can be accurately approximated by the predictions for a wire of infinite stiffness.

I. Introduction

IT has been shown[1] that wires towed behind re-entry vehicles can fail in tension at relatively low stress levels, because even at altitudes above 300 kft, aerodynamic heating can raise the wire temperature to levels at which its mechanical properties are significantly degraded. Prior to atmospheric re-entry, such wires may have random orientations, with angular displacements, relative to the velocity vector, up to 180°. Upon encountering aerodynamic resistance, these wires begin a damped periodic motion that is essentially two dimensional in the plane defined by the wire initial orientation and the velocity vector. This motion includes a large amplitude pendulum motion superimposed on a vibrational motion induced by deployment and attachment reaction forces.

The small deflection (linearized) vibrational behavior of a towed wire has been analyzed,[1,2] however, the amplitude of the small deflection motion is proportional to the initial deflection assumed. This nonlinear large deflection solution was developed to generate initial conditions for linearized solutions in which stresses and aerodynamic heating are coupled.

Wires typically experience large deflections (i.e., small angle approximations are invalid) only at attitudes above 300 kft. At these altitudes the mean free path of the air molecules is greater than an inch and therefore much greater than the diameter of any wires of interest. Consequently, aerodynamic forces at these altitudes must be calculated using free-molecule flow expressions.

In this paper, the large deflection motion of a towed wire of finite stiffness exposed to free-molecule aerodynamic drag is analyzed using nonlinear beam theory. The motion predicted by this method is then compared to the motion predicted for a rigid (infinite stiffness) wire. It is shown that for the particular cases studied, the rigid wire provides a good approximation to the finite stiffness wire motion.

Numerous papers have been written on the nonlinear response of thin elastic beams.[3-8] Eringen[3] formulates the nonlinear equations employing a fixed inertial frame of reference and a Lagrangian description of motion. Using a perturbation expansion, a solution is obtained in terms of the ratio of rotational to translational inertia for a simply supported uniform beam. Nayfeh uses the method of multiple scales to analyze the nonlinear transverse vibrations of transverse shear and rotary inertia. A variety of boundary conditions is investigated. Wagner[5] and Aravamudan and Murthy[6] using energy principles formulate a nonlinear problem considering both longitudinal and transverse inertia.

In this analysis it is assumed that the beam, or wire, is trailing behind a rigid forebody so massive that coupling between its motion and the motion of the wire is negligible. The initial position of the wire is arbitrary, and the solution obtained is valid for arbitrarily large deflection.

II. Equations of Motion

The principle of virtual work is used in the present formulation. A fixed inertial reference frame and a Lagrangian description of motion are employed assuming: 1) all motion and forces lie in the x-z plane; 2) the beam is thin, its unstrained configuration is straight, and it has a uniform cross-section that is symmetric with respect to both the y and z axes; 3) transverse sections, initially plane and normal to the beam axis, remain plane and normal after deformation; 4) the amplitudes are large, but the strains are small, such that $ds=(1+\epsilon)dx\cong dx$; and 5) the normal stress σ_{zz} is small compared to σ_{xx}, and its contribution to the strain energy is negligible.

A set of coordinates (u,w), as shown in Fig. 1, represents the components of displacements of the beam centerline from its neutral position. A third coordinate, z, represents the distance, measured normal to the beam centerline to any fiber under investigation. A second set of coordinates (U,W) represents the components of displacement of that beam fiber from its neutral position.

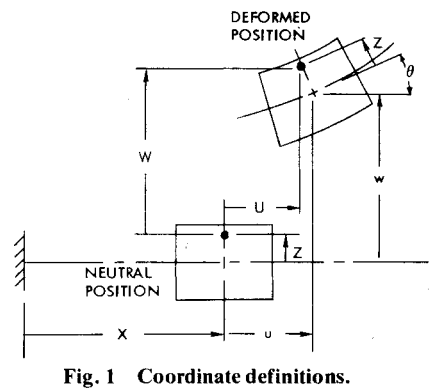

Fig. 1 Coordinate definitions.

Received Jan. 26, 1976; revision received Nov. 12, 1976.
Index categories: Entry Vehicle Dynamics and Control, Aeroelasticity and Hydroelasticity.

*Presently at Department of Engineering, California State University at Fullerton.
†Engineering Associate.

The displacements for the deformation of a flexible and extensible thin beam are given by

$$U = u - z\sin\theta \tag{1a}$$

$$W = w + z(\cos\theta - 1) \tag{1b}$$

where the angle θ is related to the displacements[9] by

$$\sin\theta = \partial w/\partial x \qquad \cos\theta = (1 + \partial u/\partial x) \tag{2}$$

The strain-displacement equation is[10]

$$\epsilon_{xx} = \frac{\partial U}{\partial x} + \frac{1}{2}\left[\left(\frac{\partial U}{\partial x}\right)^2 + \left(\frac{\partial W}{\partial x}\right)^2\right] \tag{3}$$

Substituting (1) into (3) gives

$$\epsilon_{xx} = \frac{\partial u}{\partial x} + \frac{1}{2}\left[\left(\frac{\partial u}{\partial x}\right)^2 + \left(\frac{\partial w}{\partial x}\right)^2\right] - z\frac{\partial \theta}{\partial x} + \frac{1}{2}z^2\left(\frac{\partial \theta}{\partial x}\right)^2 \tag{4}$$

Since the beam is assumed thin, the term $z^2(\partial\theta/\partial x)^2$ is small compared to $z(\partial\theta/\partial x)$ and, hence, is neglected. Thus, the strain displacement relation used is

$$\epsilon_{xx} = \epsilon - z\partial\theta/\partial x \tag{5}$$

where

$$\epsilon = \frac{\partial u}{\partial x} + \frac{1}{2}\left[\left(\frac{\partial u}{\partial x}\right)^2 + \left(\frac{\partial w}{\partial x}\right)^2\right] \tag{6}$$

From (2) one finds

$$\frac{\partial \theta}{\partial x} = \left(1 + \frac{\partial u}{\partial x}\right)\frac{\partial^2 w}{\partial x^2} - \frac{\partial^2 u}{\partial x^2}\frac{\partial w}{\partial x} \tag{7}$$

The principle of virtual work with the introduction of damping forces can be stated

$$\int_{t_1}^{t_2}\left[\delta S + \delta V - \delta T\right]dt + \int_{t_1}^{t_2}\int_0^L\left[\gamma_x \dot{u}\delta u + \gamma_y \dot{w}\delta w\right]dx\,dt = 0 \tag{8}$$

where S is the strain energy, T the kinetic energy, V is the work of external forces, and γ_x and γ_y are viscous damping constants. The kinetic and strain energy are;

$$T = \frac{1}{2}\int_V \rho\left[(\dot{U})^2 + (\dot{W})^2\right]dV \tag{9a}$$

$$S = \frac{1}{2}\int_v \sigma_{xx}\epsilon_{xx}\,dV \tag{9b}$$

where ρ is material density and for a linear elastic material

$$\sigma_{xx} = E\epsilon_{xx}$$

Substituting (1) into the above and neglecting the rotary inertia term yields

$$T = \frac{1}{2}\int_o^L m\left[(\dot{u})^2 + (\dot{w})^2\right]dx \tag{10a}$$

$$S = \frac{1}{2}\int_o^L E\left[A\epsilon^2 + I\left(\frac{\partial\theta}{\partial x}\right)^2\right]dx \tag{10b}$$

in which m represents mass per unit length.

The general expression for the work of the external forces, V is:

$$V = -\int_o^L (F_x u + F_z w)\,dx \tag{11}$$

Taking the variation of (9), (10), and (11) with respect to displacements while holding force terms constant, substituting into (8) and integrating by parts, yields an equation of the form

$$\int_{t_1}^{t_2}\int_o^L\left[f_1(u,w,x,t,F_x)\,\delta u + f_2(u,w,x,t,F_z)\,\delta w\right]dx\,dt = 0 \tag{12}$$

Since the differentials δu and δw are independent, the functions f_1 and f_2 must both be identically zero yielding the following equations of motion

$$m\ddot{u} + \gamma\dot{u} - EI\left[\frac{\partial^3 w}{\partial x^3}\left\{5\left(1 + \frac{\partial u}{\partial x}\right)\frac{\partial^2 w}{\partial x^2} - \frac{\partial^2 u}{\partial x^2}\frac{\partial w}{\partial x}\right\} - 4\frac{\partial^2 w}{\partial x^2}\frac{\partial^3 u}{\partial x^3}\frac{\partial w}{\partial x} + \frac{\partial w}{\partial x}\left(1 + \frac{\partial u}{\partial x}\right)\frac{\partial^4 w}{\partial x^4} - \left(\frac{\partial w}{\partial x}\right)^2\frac{\partial^4 u}{\partial x^4}\right] - EA\left[3\frac{\partial u}{\partial x}\frac{\partial^2 u}{\partial x^2} + \frac{3}{2}\left(\frac{\partial u}{\partial x}\right)^2\frac{\partial^2 u}{\partial x^2} + \frac{\partial^2 u}{\partial x^2} + \frac{1}{2}\frac{\partial^2 u}{\partial x^2}\left(\frac{\partial w}{\partial x}\right)^2 + \left(1 + \frac{\partial u}{\partial x}\right)\frac{\partial w}{\partial x}\frac{\partial^2 w}{\partial x^2}\right] - F_x = 0 \tag{13a}$$

$$m\ddot{w} + \gamma\dot{w} + EI\left[\frac{\partial^3 u}{\partial x^3}\left\{\left(1 + \frac{\partial u}{\partial x}\right)\frac{\partial^2 w}{\partial x^2} - 5\frac{\partial^2 u}{\partial x^2}\frac{\partial w}{\partial x}\right\} + 4\frac{\partial^2 u}{\partial x^2}\left(1 + \frac{\partial u}{\partial x}\right)\frac{\partial^3 w}{\partial x^3} - \left(1 + \frac{\partial u}{\partial x}\right)\frac{\partial w}{\partial x}\frac{\partial^4 u}{\partial x^4} + \left(1 + \frac{\partial u}{\partial x}\right)^2\frac{\partial^4 w}{\partial x^4}\right] - EA\left[\frac{3}{2}\left(\frac{\partial w}{\partial x}\right)^2\frac{\partial^2 w}{\partial x^2} + \left(1 + \frac{\partial u}{\partial x}\right)\frac{\partial w}{\partial x}\frac{\partial^2 u}{\partial x^2} + \frac{\partial u}{\partial x}\frac{\partial^2 w}{\partial x^2} + \frac{1}{2}\left(\frac{\partial u}{\partial x}\right)^2\frac{\partial^2 w}{\partial x^2}\right] - F_z = 0 \tag{13b}$$

Equations (13) are the transverse and longitudinal equations of motion for a thin beam. The boundary conditions as obtained from the variational expression can be written as:

Axial Strain:

$$\frac{\partial u}{\partial x} + \frac{1}{2}\left[\left(\frac{\partial u}{\partial x}\right)^2 + \left(\frac{\partial w}{\partial x}\right)^2\right] = 0 \tag{14a}$$

Shear:

$$\frac{\partial^3 u}{\partial x^3}\frac{\partial w}{\partial x} - \frac{\partial^3 w}{\partial x^3}\left(1 + \frac{\partial u}{\partial x}\right) = 0 \tag{14b}$$

Moment:

$$\frac{\partial^2 u}{\partial x^2}\frac{\partial w}{\partial x} - \frac{\partial^2 w}{\partial x^2}\left(1 + \frac{\partial u}{\partial x}\right) = 0 \tag{14c}$$

III. Numerical Methods

The beam is divided into equal-length elements. At every calculation step, the two components of acceleration for each

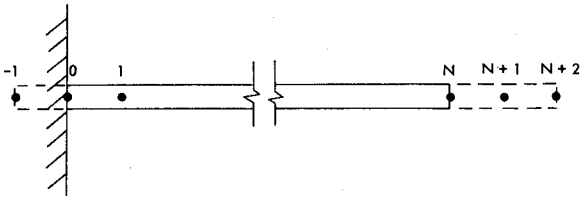

Fig. 2 Fictitious point positions.

point on the beam are calculated by evaluating Eqs. (13a) and (13b) using the instantaneous values of velocity and displacement. These accelerations are then integrated independently using a forward difference technique to obtain new velocities and positions for the points. To provide direct control over numerical stability, a variable time step is used. The time step is determined to be that time step that allowed the fastest moving point on the beam to move a preselected distance.

Boundary conditions (BC's) are enforced by creating fictitious points past each end of the beam, as shown in Fig. 2. Since there are three BC's, it is possible to establish both coordinates for points $N+1$ and one coordinate for points $N+2$ and -1. After advancing the points on the beam using the equations of motion, the coordinates of the fictitious points are determined. Values for these coordinates are found so that derivatives at the two ends of the beam, including the fictitious points in their calculation, satisfy the BC equations.

While the fixed end BC's are relatively straightforward, the free end BC's are not. Consequently, two different independent methods for solving the free end BC's have been developed, and the results have been compared. The methods are: 1) forward difference BC solution, and 2) the simultaneous BC solution. Both method use finite difference expressions for some or all of the derivatives in the BC equations so that the unknown fictitious point coordinates appear explicitly. The equations then can be solved for those coordinates. The first method operates on only one equation at a time and breaks down numerically only one of the derivatives. Linear expressions for each fictitious point coordinate are determined and evaluated easily by using old values for the other derivatives and new values for coordinates. The second method is more difficult and requires all derivatives in all three BC equations be expressed numerically and solved simultaneously for the three coordinates. The Appendix discusses these techniques in more detail.

In the solution for the fixed end, the base point zero always has coordinates (0.0,0.0). Following linear theory, point -1 is assigned: clamped: $w_{-1}=w_1$; pinned: $w_{-1}=-w_1$.

IV. Results

The previous expressions were incorporated into a finite difference computer code. To verify this solution technique, two test cases were evaluated. The first case represents a wire initially under axial tension, instantaneously released. The analytic solution[11] for the free end deflection history is a triangular wave, and the code predicts exactly this behavior. The second case treated was the free transverse vibration of a steel wire. The wire was assumed clamped at the fixed end and initially linearly deflected through a small angle. Figure 3 compares the motion predicted by this method to that predicted by a small deflection (linearized) method, and in addition, the true primary natural frequency measured in the laboratory is shown. The agreement between the cases is good, and both correlate well with the measured natural frequency. Even though no quantitative measurements could be obtained, the strong higher harmonic motion predicted by the codes was also observed in the laboratory.

Although no problems were encountered with the case describing axial vibration along the x axis, severe axial stability problems arose while analyzing coupled axial and

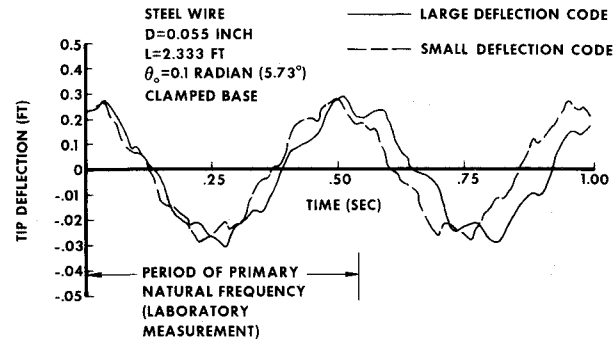

Fig. 3 Large and small deflection codes comparison.

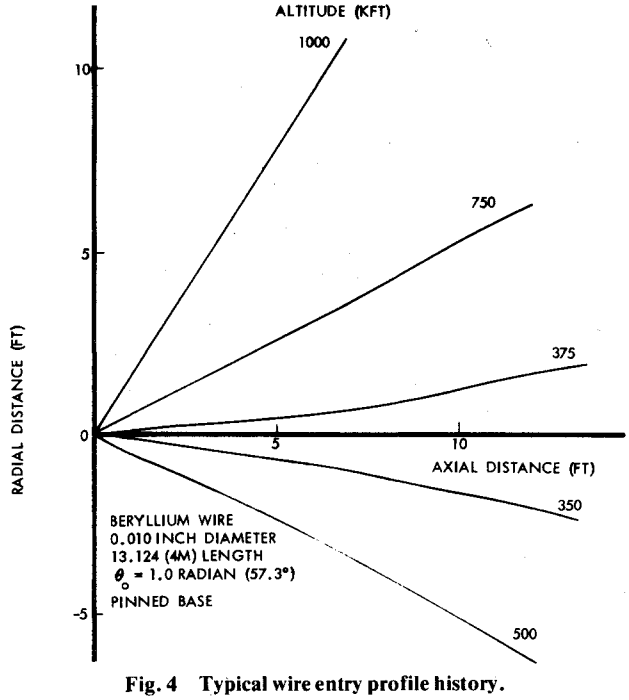

Fig. 4 Typical wire entry profile history.

transverse motion. Axial vibrations were found to be amplified and could not be stabilized by changing either the computing time step or the element length. It was found, however, that these vibrations could be controlled[12] by employing an artificially low modulus of elasticity in the axial direction. Damping in the axial direction also was tried, but appeared to be counterproductive, so for all further analyses both axial and lateral damping coefficients were set to zero. Stability appeared to increase monotonically as the axial modulus was reduced, so that most calculations were ultimately made with the smallest possible modulus that would prevent the wire from stretching unrealistically. Typically, axial moduli that were five orders of magnitude smaller than the actual modulus of the material were used.

The reason for this stability problem is felt to be truncation errors in the numerical solution of the equations. Transverse deflections are on the order of the total length of the wire, while axial deflections (using the true modulus) are many orders of magnitude less. In solving the coupled problem, the truncation error in evaluating derivatives can easily be larger than the axial deflection, thereby introducing meaningless axial deflections and forces. This argument is supported by the fact that this instability is controlled by reducing the axial modulus. One of the primary effects of the lower modulus is proportionally increased axial deflections, so that the axial deflections become much larger than the truncation errors.

As the molecular mean free path is much greater than the wire diameters considered for all altitudes studied, free

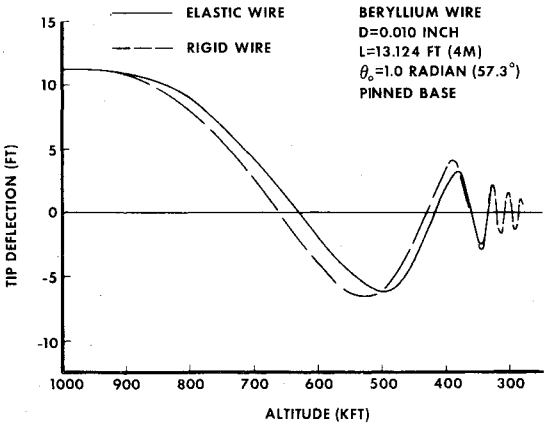

Fig. 5 Comparison between elastic and rigid wire analyses.

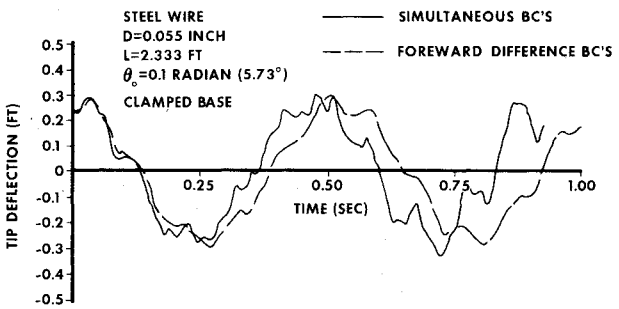

Fig. 6 Boundary-condition solution comparison.

molecule flow expressions were used. For simplicity, an accommodation coefficient (fraction of freestream momentum absorbed) of unity was assumed. Note that since the reflected molecule velocity is then zero, the aerodynamic force is applied only in the axial direction.

It was found that for the very thin wires evaluated, bending forces were much smaller than aerodynamic forces so that there was little difference between the motion predicted using the pinned and clamped boundary conditions. In addition, since the forebody will have a motion of its own induced by its aerodynamic drag, the pinned analysis provides the better simulation of its physical analog. Consequently, the majority of the analyses were performed using the pinned boundary conditions. Figure 4 shows a typical profile history for an entry analysis initiated at an altitude of 1000 kft with an initial angular displacement of 1.0 rad. It is seen that due to the uniformity and the low magnitude of the aerodynamic drag, the wire remains nearly straight. Consequently, the adequacy of an infinite stiffness (rigid) wire analysis was evaluated. The motion of a rigid wire with one pinned end in free molecule flow is given by

$$\ddot{\theta} = \text{moment}/I_\rho \tag{15a}$$

$$= \frac{-3}{2}\,\frac{\rho_\infty v_\infty^2 \,\text{Sin}^2\theta}{mL} \tag{15b}$$

The equations of motion in the wire motion computer code were replaced by Eq. (15) and Fig. 5 compares the tip deflection histories predicted with this rigid wire analysis to that predicted by the elastic wire analysis above. It is seen that for the particular wire analyzed (over 15,000 diam in length), the two solutions differ only slightly. The difference in the tip position predicted by the two methods is due primarily because the tip of the elastic rod lags behind its centroid.

The changes in amplitude and frequency predicted by both methods as the wire descends in altitude are due to the fact that the atmospheric density, and therefore the force potential, is increasing approximately exponentially.

V. Conclusions

Equations of motion were derived using the principle of virtual work and were incorporated into a computer code for analyzing the large deflection re-entry dynamic motion of a thin wire. The use of an artifically low elastic modulus in the axial direction was necessary to obtain stable solutions to coupled axial and transverse motion problems. Employing either of two different boundary-condition formulations, this technique provided a description of the dynamic motion of an elastic wire that compares well with experiment.

Appendix: Boundary-Condition Solutions

A. Forward Difference Free End Boundary-Condition Solution

To allow incorporation of the forward difference boundary-condition (BC) solution at the free end, the following first order expressions were used for first and second derivatives of both u and w

$$u_i' = (u_{i+1} - u_{i-1})/2\Delta$$

$$u_i'' = (u_{i+1} - 2u_i + U_{i-1})/2\Delta^2$$

The BC solution begins by solving the axial strain BC for u' in terms of w'

$$u' = -1 \pm \sqrt{1 - w'^2}$$

in which the (+) is required for angles in quadrants I and IV (0° ±90°), and the (−) is required in II and III (180° ±90°). The u coordinate of point N + 1 then is found by expressing u' numerically and solving

$$u_{N+1} = u_{N-1} + 2\Delta(-1 \pm \sqrt{1 - w'^2})$$

Similarly, the moment BC is solved for w'', which then is expressed numerically. The resultant expression is solved for the w coordinate of point N + 1

$$w_{N+1} = 2w_N - w_{N-1} + \Delta^2 \frac{u'' w'}{1 + u'}$$

Similar operations on w''' in the shear BC yields an expression for the w coordinate of point N + 2

$$w_{N+2} = w_{N-2} - 2w_{N-1} + 2w_{N+1} + 2\Delta^3 \frac{u''' w'}{1 + u'}$$

The u coordinate of point N + 2 is calculated trigonometrically by assuming that the beam centerline distance between points N and N + 1 equals the beam centerline distance between points N + 1 and N + 2.

In practice, all spatial derivatives are determined and then used as known values in integrating the equations of motion to calculate new coordinates along the wire at the end of the time step. Following this, the sequence of calculations described above for locating the fictitious points is executed. Consequently, the free end fictitious points are located using coordinates valid at the end of the time step with derivatives valid at the beginning of the time step.

B. Simultaneous Free End BC Solution

In this formulation, a single fictitious point, only requiring the w coordinate, is used. The unknowns to be found are this value and the two coordinates of the end point of the wire. Derivatives of the variable u in the BC equations are approximated by backwards difference formulas. Derivatives of w are approximated by special 3/4 difference formulas using the values w_{N+1}, w_N, w_{N-1}, w_{N-2}, and w_{N-3} (Table 1). Note that derivatives used in the equations of motion at point N − 1 will be approximated by central difference in w and the special 3/4 difference in u. Substituting the finite difference

Table 1 Finite difference formulas used to approximate derivatives[a]

Derivative	Central difference	Backwards difference	Special 3/4 difference
g_i'	$\frac{g_{i-2}-8g_{i-1}+8g_{i+1}-g_{i+2}}{12h}$	$\frac{11g_i-18g_{i-1}+9g_{i-2}-2g_{i-3}}{6h}$	$\frac{3g_{i+1}+10g_i-18g_{i-1}+6g_{i-2}-g_{i-3}}{12h}$
g_i''	$\frac{-g_{i-2}+16g_{i-1}-30g_i+16g_{i+1}-g_{i+2}}{12h^2}$	$\frac{2g_i-5g_{i-1}+4g_{i-2}-g_{i-3}}{h^2}$	$\frac{11g_{i+1}-20g_i+6g_{i-1}+4g_{i-2}-g_{i-3}}{12h^2}$
g_i'''	$\frac{-g_{i-2}+2g_{i-1}-2g_{i+1}+g_{i+2}}{2h^3}$	$\frac{g_i-3g_{i-1}+3g_{i-2}-g_{i-3}}{h^3}$	$\frac{3g_{i+1}-10g_i+12g_{i-1}-6g_{i-2}+g_{i-3}}{2h^3}$
g_i^{iv}	$\frac{g_{i-2}-4g_{i-1}+6g_i-4g_{i+1}+g_{i+2}}{h^4}$	----------	$\frac{g_{i+1}-4g_i01i-1-4g_{i-2}+g_{i-2}}{h^4}$

[a] Derivaties of g at the point i. Distance between grid points $= h$.

formulas into the BC equations yields three nonlinear algebraic equations for the unknown w_{N+1}, w_N, and u_N.

$$f_1(w_{N+1}, w_N, u_N) = 0$$

$$f_2(w_{N+1}, w_N, u_N) = 0$$

$$f_3(w_{N+1}, w_N, u_N) = 0$$

To solve these equations, a Newton's method is used. The method consists of an iterative scheme, solving the Jacobian matrix equation for correction terms. At the $K+1^{th}$ iteration, new values for the three unknowns are found from

$$-\begin{Bmatrix} f_1 \\ f_2 \\ f_3 \end{Bmatrix}^K = \begin{bmatrix} \partial f_1/\partial w_{N+1} & \partial f_1/\partial w_N & \partial f_1/\partial u_N \\ \partial f_2/\partial w_{N+1} & \partial f_2/\partial w_N & \partial f_2/\partial u_N \\ \partial f_3/\partial w_{N+1} & \partial f_3/\partial w_N & \partial f_3/\partial u_N \end{bmatrix} \times \begin{Bmatrix} w_{N+1}^{K+1} - w_{N+1}^K \\ w_N^{K+1} - w_N^K \\ N_u^{K+1} - u_N^K \end{Bmatrix}$$

The convergence criterion used is

$$\sqrt{f_1^2+f_2^2+f_3^2} < 10^{-5}$$

Figure 6 compares the predictions obtained using the two BC solutions for the free vibration of the steel wire discussed above. The results are similar: however, the simultaneous BC solution approximately doubles the computer time required due to the number of additional arithmetic operations.

Acknowledgment

This work was performed under Massachusetts Institute of Technology, Lincoln Laboratory Purchase Order C-980.

References

[1] "Trailing Wire Design Study Final Report," Prototype Development Associates, Santa Ana, Calif., Report TR 1037-00-04, June 1975.

[2] Brown, J., "Stresses in Towed Cables During Reentry," *Journal of Spacecraft*, Vol. 12, Sept. 1975, pp. 524-527.

[3] Eringen, A.C., "On the Nonlinear Vibration of Elastic of Bars," *Quarterly Journal of Applied Mathematics*, Vol. 9, 1952, pp. 361-369.

[4] Nayfeh, A. H., "Nonlinear Transverse Vibrations of Beams with Properties that Vary Along the Length," *Journal of the Acoustical Society of America*, Vol. 53, 1973, pp. 766-770.

[5] Wagner, H., "Large Amplitude Free Vibration of a Beam," *Journal of Applied Mechanics*, Vol. 32, 1965, pp. 887.

[6] Aravamundan, K. S. and Murthy, P. N., "Nonlinear Vibration of Beams with Time-Dependent Boundary Conditions," *International Journal of Nonlinear Mechanics*, Vol. 8, 1973, pp. 195-212.

[7] Evensen, D. E., "Nonlinear Vibration of Beams with Various Boundary Conditions," *AIAA Journal*, Vol. 6, Feb. 1968, pp. 370-372.

[8] Bennett, J. A. and Eisley, J. G., "A Multiple-Degree of Freedom Approach to Nonlinear Beam Vibrations," *AIAA Journal*, Vol. 8, April 1970, pp. 734-740.

[9] Novozhilov, V. V., *Foundations of the Nonlinear Theory of Elasticity*, Graylock Press, Rochester, New York, 1953.

[10] Stoker, J. J., *Nonlinear Elasticity*, Gordon and Breach, New York, 1968.

[11] Churchill, R. V., *Operational Mathematics*, McGraw-Hill, New York, 1958, pp.121-122.

[12] Kettner, D. and Hyland D., personal communication, MIT Lincoln Laboratory, Cambridge, Mass. 1975.